

See discussions, stats, and author profiles for this publication at: <https://www.researchgate.net/publication/255763149>

‘Pourbaix sensors’: a new class of fluorescent pE–pH molecular AND logic gates based on photoinduced electron transfer

ARTICLE *in* NEW JOURNAL OF CHEMISTRY · DECEMBER 2012

Impact Factor: 3.09 · DOI: 10.1039/C2NJ40732A

CITATIONS

6

READS

11

2 AUTHORS, INCLUDING:



David C Magri

University of Malta

34 PUBLICATIONS 1,209 CITATIONS

SEE PROFILE

LETTER

'Pourbaix sensors': a new class of fluorescent pE–pH molecular AND logic gates based on photoinduced electron transfer†

Cite this: *New J. Chem.*, 2013, **37**, 148

Received (in Montpellier, France)
16th August 2012,
Accepted 10th October 2012

Thomas J. Farrugia and David C. Magri*

DOI: 10.1039/c2nj40732a

www.rsc.org/njc

A novel anthracene-based molecular AND logic gate displays a fluorescence output in methanol after chemical oxidation of the ferrocene moiety with Fe(III) and protonation of the tertiary amine. This new class of probes could have practical applications in corrosion science and living cell imaging.

Molecular and supramolecular information processing continues to be a vibrant progressive research field.¹ Since the inception of the first two-input molecular AND logic gate by de Silva *et al.* two decades ago,² many types of switchable logic gates and arrays responsive to two or more physical and/or chemical signals have been successfully demonstrated using various controllable stimuli including light, pH, ions and redox potential.³ Of these possible combinations of stimuli, there are few examples of molecular logic gates with a redox switching input and an optical output.⁴

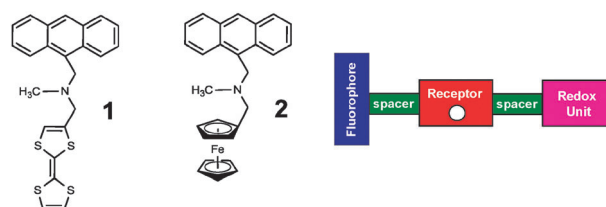
Combining concepts from photoinduced electron transfer (PET) pH sensors⁵ and redox-fluorescent pE switches,⁶ we define a new class of sensor, which simultaneously monitor the pE and pH in solution according to the AND logic.⁷ Molecular AND logic gates driven by potential and protons as inputs and an optical output could have practicality in environmental and biological applications. For instance, the relationship between the potential and proton concentration in aqueous solution is of paramount importance in the electrochemistry of metal species as well as in corrosion science, mining and geochemistry. In fact, a diagram relating the thermodynamic stability of the various states of an element or compound as a function of pE and pH is known universally as a Pourbaix diagram.⁸

Another potential realm of practicality for sensors combining pH and pE could be in cell biology. Fluorescent indicators are routinely used for measuring the intracellular pH in the cytosol

and organelles of live cells.⁹ PET pH sensors with weak nitrogen bases are known to selectively concentrate in acidic organelles on protonation, and unlike most commercially available pH indicators, they become more fluorescent in an acidic environment.¹⁰ With regard to cytotoxicity probes, the commercially available Redox-Sensor red CC-1 stain and tetrazolium salts are routinely used for detecting, among many species, the redox potential in cell compartments.¹⁰ Transition metals, notably free iron as Fe(II), are a potential cause of cytotoxicity in cells because they catalyze the formation of reactive oxygen species.¹¹ However, despite there being molecular probes for specifically monitoring the pH or the pE in living cells, to the best of our knowledge, no probe currently exists that can simultaneously probe both the pH and pE in living cells. Such probes could be of immense importance as high concentrations of protons and redox-active iron have been linked to various cancers, such as colorectal and liver cancer.¹²

Previously we reported the characterization and logic characteristics of **1** in acetonitrile.⁷ Using cyclic voltammetry, the standard potentials of the various components were measured in order to gain insight into the electron transfer thermodynamics. The AND logic characteristics were demonstrated using bulk electrolysis, hence with an applied voltage at an electrode, as well as with the chemical oxidant Fe(III).

In this communication, we elaborate on the concept with a new molecular sensor modulated by pE and pH according to the AND



Scheme 1 The molecular structures of the pE–pH fluorescent AND logic gates **1** and **2** and a cartoon schematic of the design principle.

Department of Chemistry, University of Malta, Msida, MSD 2080, Malta.

E-mail: david.magri@um.edu.mt; Fax: +356 2340 3320; Tel: +356 2340 2276

† Electronic supplementary information (ESI) available. See DOI: 10.1039/c2nj40732a

logic. The logic gates **1** and **2** are designed on a modular approach based on the principles of PET according to a fluorophore-spacer-receptor-spacer-redox donor format (Scheme 1).⁷ An enhanced fluorescence output is exhibited upon oxidation with Fe(III) and at elevated proton concentrations. Common to both **1** and **2** is an anthracene fluorophore connected to a tertiary amine receptor for H⁺, which is connected to a redox active donor. Logic gate **1** incorporates tetrathiafulvalene (TTF), a popular motif in supramolecular chemistry. In **2** the redox donor is ferrocene, a common motif in sensor research. Despite the standard potentials of TTF and ferrocene being nearly identical, the fact that TTF has two oxidized states *versus* one for ferrocene has a dramatic effect on the electron transfer pathways, and hence the molecular response to excess Fe(III). Notably, while the fluorescence of **1** is quenched in the presence of more than one equivalent of Fe(III), our novel logic gate **2** remains fluorescent in the presence of excess equivalents of Fe(III).

The logic gate **2** was synthesized by reductive amination of (*N*-methyl)aminomethylantracene and ferrocene carboxaldehyde with sodium triacetoxy borohydride.¹³ The crude product was recrystallized from methanol to yield an orange solid in 21% yield. The compound was characterised using standard techniques including ¹H, ¹³C and ¹³C DEPT NMR spectroscopy as detailed in the ESI† (Fig. S1–S4).

The logic gate **2** was first studied in acetonitrile for direct comparison with **1** and then in methanol using UV-visible absorption. In both acetonitrile and methanol well-defined vibrational peaks characteristic of the anthracene chromophore are observed at 349, 365 and 386 nm in acetonitrile with molar extinction coefficients of 6400, 9900 and 9500 cm^{−1} mol^{−1} L. The analogous values in methanol are 7800, 12 000 and 11 400 cm^{−1} mol^{−1} L (Fig. S4, ESI†). Addition of 1 mM methanesulfonic acid results in a bathochromic shift of 4 nm as observed with **1**.⁷ Addition of Fe(III) results in a gradual increase in the absorbance due to the yellow-coloured Fe(III) ion absorbing within the same region, which results in gradual loss of the anthracene fine structure. However, despite the increase in absorbance due to Fe(III) the fluorescence output increases substantially, rather than decreasing due to inner filter effects.

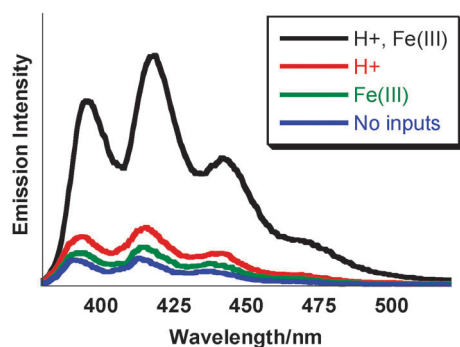


Fig. 1 Fluorescence spectra of 10^{−5} M **2** in methanol excited at 365 nm. An enhanced fluorescence signal is observed after oxidation of the ferrocene moiety with Fe(III) and protonation of the tertiary amine.

Table 1 Truth table for the AND logic gate **2**^a

Input ₁ (H ⁺) ^b	Input ₂ (Fe ³⁺) ^c	Output emission (φ _F) ^d
0 (low)	0 (low)	0 (low, 0.001)
0 (low)	1 (high)	0 (low, 0.002)
1 (high)	0 (low)	0 (low, 0.004)
1 (high)	1 (high)	1 (high, 0.018) ^e

^a 10^{−5} M **2** excited at 365 nm in methanol. ^b High input level 0.1 mM methanesulfonic acid. Low input level no acid. ^c High input level 0.1 mM iron(III) sulphate pentahydrate. Low input level no iron added. ^d Relative φ_F measured with reference to anthracene in aerated ethanol (φ_F = 0.27).¹⁷ Output level high when φ_F > 0.006. ^e Corrected for inner filter effects.

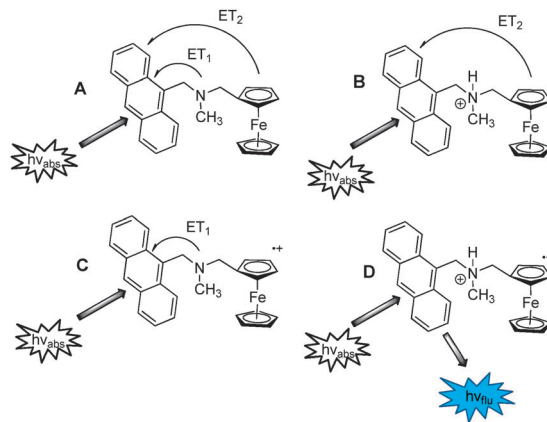


Fig. 2 Pictorial form of the truth table of the AND logic gate **2** illustrating the four states and the electron transfer deactivation pathways.

The digital logic characteristics of **2** were investigated in both acetonitrile and methanol by observing the fluorescence spectra under four experimental conditions. In the presence of excess methanesulfonic acid and Fe(III) the fluorescence output in methanol is significantly high relative to the other three input conditions as shown in Fig. 1. In the ‘off’ states, the fluorescence output is low either due to PET from the amine and/or PET from ferrocene to the excited fluorophore. The specific details in methanol including the relative quantum yields of fluorescence are given in Table 1.

The driving forces for the various PET pathways can be predicted from the Weller equation.¹⁴ These are illustrated in Fig. 2. PET from the amine to the excited state anthracene is spontaneous with a Δ*G*_{PET} of −0.1 V (Fig. 2C). Addition of acid protonates the electron lone pair thus preventing PET from the amine, but not from ferrocene. PET from ferrocene to the excited state fluorophore is favourable with a driving force of −1.0 V (Fig. 2B). In comparison, PET from the ferrocenium radical cation to the excited anthracene is not feasible as the driving force for PET is uphill by 0.6 V.¹⁵ Only when the input conditions result in the tertiary amine being protonated and the redox donor oxidized to the radical cation is a significant fluorescence enhancement observed.

As observed with other anthracene–ferrocene sensors,^{4b,16} and similar to our past study of **1**, the resulting quantum yield in the ‘on’ state is modest (Table 1, entry 4).⁷ The high output

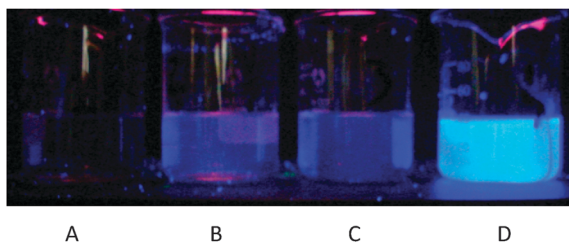


Fig. 3 Fluorogenic response of **2** (10^{-5} M) in methanol irradiated with a handheld UV lamp at 365 nm in a dark cabinet. The labels correspond to those in Fig. 2. See footnotes in Table 1 for specific experimental conditions.

emission of 0.018 is an order of magnitude lower than the reference quantum yield of 0.27 for anthracene in ethanol.¹⁷ This is possibly due to a competing PET from the excited anthracene to ferrocenium which has a driving force of -1.5 V. A negative driving force of this magnitude suggests that electron transfer occurs in the Marcus inverted region.¹⁸ The present case suggests the possibility of a residual back PET in the 'on' state that occurs in the opposite direction of that from the neutral redox donor. However, it is also possible that spectral overlap between the emission spectrum of anthracene and the absorption spectrum of the ferrocenium radical cation provides an alternative deactivation pathway *via* energy transfer.¹⁹ As shown in Fig. 3, despite the modest fluorescence quantum yields, the output states of AND logic gate **2** are visually acute to the naked eye under UV irradiation.

Absorption and fluorescence titrations were carried out in acetonitrile and methanol. One set of titration experiments involved titrating **2** with each individual input, and another set of titrations was conducted in the presence of one input in excess. The fluorescence output in methanol increases in the presence of both inputs irrespective of the order in which they are added to solution. On increasing the acid concentration, an increase in the fluorescence is observed, albeit with greater intensity in methanol, which resulted in a much better defined spectrum as illustrated by Fig. 1. The binding constants $\log \beta_{H^+}$ were determined using the Henderson–Hasselbalch equation adopted for fluorimetric analysis.^{5a} The measured $\log \beta_{H^+}$ values were 5.3 and 4.6 in acetonitrile and methanol, respectively, which are consistent with values for related anthracene-spacer-amine-type molecular logic gates.^{2,20} Water soluble anthracene-based sensors with a similar ammonium group have a pK_a of 7.8.²¹ Hence the usable pH range of **2** would be anticipated to be near-neutral pHs of 7.0–8.5. The concentration range examined for Fe(III) was between 10 and 100 μ M.

An exciting outcome from this study is that the fluorescence of **2** is enhanced, rather than quenched, in the presence of excess Fe(III). This is contrary to **1** which exhibited a fluorescence decrease upon addition of more than one equivalent of Fe(III).^{6,7} This is rather interesting as the only difference between **1** and **2** is the nature of the redox unit. The 'on' state for **2** occurs when the ferrocene moiety is oxidized to the radical cation, whereas with **1** the optimal 'on' state occurs when the TTF is oxidized to its dication.⁷

In summary, we have synthesized a novel fluorescent AND logic gate for pE and pH based on the principles of PET. Protonation of the amine and oxidation of ferrocene to ferrocenium results in a five-fold fluorescence enhancement in methanol. Unlike **1** which in the presence of acid undergoes a fluorescence 'turn-off' response in the presence of more than one equivalent of Fe(III), **2** is observed to undergo a 'turn-on' response. Further work aims at designing pE–pH fluorescent 'Pourbaix sensors' that operate in aqueous solution for practical environmental and biological applications.

Experimental

Instrumentation

^1H , ^{13}C and ^{13}C DEPT NMR spectra were recorded at room temperature on a Bruker AM 250 NMR spectrometer equipped with a $^1\text{H}/^{13}\text{C}$ 5 mm dual probe at 250.1 and 62.9 MHz, respectively, with CDCl_3 as the solvent. Spectra are reported in ppm *versus* tetramethylsilane ($\delta = 0.00$) for ^1H NMR and CDCl_3 ($\delta = 77.00$) for ^{13}C NMR. The infra-red spectrum was recorded on a Shimadzu IR-Affinity 1 spectrometer as a thin film from dichloromethane between NaCl plates. Electron impact (EI) spectra were obtained on a Thermo Finnigan Trace DSQ spectrometer. The melting point was recorded on a Griffin melting point apparatus and is uncorrected. UV-visible absorption and fluorescence spectra were recorded on a Jasco V-650 spectrophotometer and a Jasco FP-8300 fluorescence spectrometer, respectively. Fluorescence experiments were performed in emission mode with the excitation and emission slit widths set at 2.5 nm.

Synthesis

The molecular AND logic gate **2** was prepared by reductive amination of (*N*-methyl)aminomethylantracene (0.20 g, 0.90 mmol) and ferrocene carboxaldehyde (0.19 g, 0.90 mmol) with sodium triacetoxyborohydride (0.26 g, 1.2 mmol) in the presence of 4 Å molecular sieves, 1,2-dichloroethane (12 mL) and a few drops of glacial acetic acid. The reaction mixture was stirred for 48 hours in the dark. The product was recovered by extracting with 30 mL of dichloromethane, which was washed four times with 10 mL of saturated sodium hydrogen carbonate solution and further three times with 10 mL of brine solution. The remaining yellow solution was evaporated under vacuum, and recrystallized from methanol to yield an orange crystalline solid. Overall yield was 21% (0.38 g); m.p. 128–130 °C; $\nu_{\text{max}}(\text{NaCl})/\text{cm}^{-1}$: 3086, 3049, 2938, 2835, 2779, 1622, 1522, 1445, 1341, 1265, 1105, 1001, 885, 860, 820, 731; $\delta\text{H}(250\text{ MHz}, \text{CDCl}_3, \text{SiMe}_4)$: 2.14 (s, 3H, NCH_3), 3.67 (s, 2H, CH_2 spacer₁), 4.11 (s, 5H, C_5H_5), 4.20 (s, 2H, upper C_5H_5), 4.31 (s, 2H, upper C_5H_5), 4.36 (s, 2H, CH_2 spacer₂), 7.39–7.50 (m, 4H, anthracene), 7.93–8.02 (m, 2H, anthracene), 8.28–8.41 (3H, m, anthracene); $\delta\text{C}(62.9\text{ MHz}, \text{CDCl}_3, \text{SiMe}_4)$: 41.9, 52.1, 58.4, 68.1, 68.5, 70.4, 83.8, 124.8, 125.1, 125.5, 127.3, 129.0, 130.7, 131.3, 131.4; m/z (EI): 220.9(72), 217.9(36), 203.9(11), 190.9(100), 177.9(56); calcd for $\text{C}_{27}\text{H}_{26}\text{FeN}$ ($\text{M}^{\bullet+}$) 420.1415, found 420.1423.

Titration

Titration was performed in 40 mL volumes of HPLC grade acetonitrile or methanol containing 10 μ M of **2**. Iron(III) sulfate

pentahydrate was used in methanol and iron(III) perchlorate in acetonitrile. Proton binding constants were determined in the presence of 100 μM iron(III) sulphate pentahydrate. Solutions of 1.25 mM methanesulfonic acid and iron(III) sulfate pentahydrate were used as the titrant.

Acknowledgements

The University of Malta (UoM) and the Department of Chemistry at UoM are acknowledged for financial support. Prof. Robert M. Borg is thanked for assistance with the acquisition of the NMR spectra.

References

- 1 *Molecular and Supramolecular Information Processing: From Molecular Switches to Logic Systems*, ed. E. Katz, Wiley-VCH Verlag, Weinheim, Germany, 2012.
- 2 A. P. de Silva, H. Q. N. Gunaratne and C. P. McCoy, *Nature*, 1993, **364**, 42.
- 3 (a) E. Katz, V. Bocharova and M. Privman, *J. Mater. Chem.*, 2012, **22**, 8171; (b) A. P. de Silva, *Chem.-Asian J.*, 2011, **6**, 750; (c) G. de Ruiter and M. E. van der Boom, *Acc. Chem. Res.*, 2011, **44**, 563; (d) J. Andréasson and U. Pischel, *Chem. Rev.*, 2010, **39**, 174; (e) U. Pischel, *Aust. J. Chem.*, 2010, **63**, 148; (f) V. Balzani, A. Credi and M. Venturi, *Chem.-Eur. J.*, 2008, **14**, 26; (g) K. Szacilowski, *Chem. Rev.*, 2008, **108**, 3481; (h) U. Pischel, *Angew. Chem., Int. Ed.*, 2007, **46**, 4026; (i) A. Credi, *Angew. Chem., Int. Ed.*, 2007, **46**, 5472; (j) A. P. de Silva and S. Uchiyama, *Nat. Nanotechnol.*, 2007, **2**, 399; (k) H. Tian, *Angew. Chem., Int. Ed.*, 2010, **49**, 4710; (l) R. Freeman and I. Willner, *Chem. Soc. Rev.*, 2012, **41**, 4067; (m) V. Balzani, M. Venturi and A. Credi, *Molecular Devices and Machines*, Wiley-VCH, Weinheim, 2nd edn, 2008.
- 4 For example: (a) R. S. Sánchez, R. Gras-Charles, J. L. Bourdelande, G. Guirado and J. Hernando, *J. Phys. Chem. C*, 2012, **116**, 7164; (b) C.-J. Fang, C.-Y. Li, X.-F. Fu, Y.-F. Yue and C.-H. Yan, *Chin. J. Inorg. Chem.*, 2008, **24**, 1832; (c) C. J. Fang, Z. Zhu, W. Sun, C. H. Xu and C. H. Yan, *New J. Chem.*, 2007, **31**, 580; (d) M. Biancardo, C. Bignozzi, H. Doyle and G. Redmond, *Chem. Commun.*, 2005, 3918; (e) T. Komura, G. Y. Niu, T. Yamaguchi and M. Asano, *Electrochim. Acta*, 2003, **48**, 631; (f) P. R. Ashton, V. Baldoni, V. Balzani, A. Credi, H. D. A. Hoffmann, M.-V. Martínez-Díaz, F. M. Raymo, J. F. Stoddart and M. Venturi, *Chem.-Eur. J.*, 2001, **7**, 3482; (g) S. Monaco, M. Semeraro, W. Tan, H. Tian, P. Ceroni and A. Credi, *Chem. Commun.*, 2012, **48**, 8652; (h) T. Gupta and M. E. van der Boom, *Angew. Chem., Int. Ed.*, 2008, **47**, 5322.
- 5 (a) R. A. Bissell, A. P. de Silva, H. Q. N. Gunaratne, P. L. M. Lynch, G. E. M. Maguire and K. R. A. S. Sandanayake, *Chem. Soc. Rev.*, 1992, **21**, 187; (b) A. P. de Silva and R. A. D. D. Rupasinghe, *J. Chem. Soc., Chem. Commun.*, 1985, 1669.
- 6 (a) L. Fabbrizzi and A. Poggi, *Chem. Soc. Rev.*, 1995, **24**, 197; (b) G. X. Zhang, D. Q. Zhang, X. F. Guo and D. B. Zhu, *Org. Lett.*, 2004, **6**, 1209.
- 7 D. C. Magri, *New J. Chem.*, 2009, **33**, 457.
- 8 M. Pourbaix, *Atlas of Electrochemical Equilibria in Aqueous Solutions*, Pergamon Press, Oxford, U.K., 1966.
- 9 J. Han and K. Burgess, *Chem. Rev.*, 2010, **110**, 2709.
- 10 I. Johnson and M. T. Z. Spence, *The Molecular Probes Handbook: A Guide to Fluorescent Probes and Labeling Technologies*, Life Technologies Corporation, U.S., 11th edn, 2010.
- 11 (a) N. C. Andrews, *Am. J. Physiol.: Cell Physiol.*, 2004, **287**, 1537; (b) D. S. Kalinowski and D. R. Richardson, *Pharmacol. Rev.*, 2005, **57**, 547.
- 12 X. Huang, *Mutat. Res.*, 2003, **533**, 153.
- 13 A. F. Abdel-Magid, K. G. Carson, B. D. Harris, C. A. Maryanoff and R. D. Shah, *J. Org. Chem.*, 1996, **61**, 3849.
- 14 A. Weller, *Pure Appl. Chem.*, 1968, **16**, 115. The driving force for PET is calculated from $\Delta G_{\text{PET}} = E_{\text{OX}} - E_{\text{RED}} - E_{\text{S}} - e^2/\epsilon r$ where E_{OX} is the oxidation potential of ferrocene (0.45 V), E_{RED} is the reduction potential of anthracene (−1.90 eV), E_{S} is the singlet excited energy of anthracene (3.20 eV) and $e^2/\epsilon r$ is the coulombic term (0.10 eV). All values are *versus* SCE.
- 15 Calculated using E_{OX} of anthracene (1.4 eV) and E_{RED} of ferrocenium (−0.45 eV).
- 16 (a) F. Sancenón, A. Benito, F. J. Hernández, J. M. Lloris, R. Martínez-Mañez, T. Pardo and J. Soto, *Eur. J. Inorg. Chem.*, 2002, 866; (b) A. Caballero, R. Tormos, A. Espinosa, M. D. Velasco, A. Tárraga, M. A. Miranda and P. Molina, *Org. Lett.*, 2004, **6**, 4599.
- 17 W. R. Dawson and M. W. Windsor, *J. Phys. Chem.*, 1968, **72**, 3251.
- 18 R. A. Marcus and N. Sutin, *Biochim. Biophys. Acta*, 1985, **811**, 265.
- 19 S. Fery-Forgues and B. Delavaux-Nicot, *J. Photochem. Photobiol., A*, 2000, **132**, 137.
- 20 A. P. de Silva, H. Q. N. Gunaratne and C. P. McCoy, *J. Am. Chem. Soc.*, 1997, **119**, 7891.
- 21 (a) J. F. Callan, A. P. de Silva and N. D. McClenaghan, *Chem. Commun.*, 2004, 2048; (b) D. C. Magri and A. P. de Silva, *New J. Chem.*, 2010, **34**, 476.